Rapid Communications

Exploring the diluted ferromagnetic p-spin model with a cavity master equation

Erik Aurell,[1,*] Eduardo Domínguez,[2] David Machado,[2] and Roberto Mulet[2,†]

[1]*KTH Royal Institute of Technology, AlbaNova University Center, SE-106 91 Stockholm, Sweden*

[2]*Group of Complex Systems and Statistical Physics, Department of Theoretical Physics, University of Havana, Cuba*

(Received 6 February 2018; published 30 May 2018)

We introduce an alternative solution to Glauber multispin dynamics on random graphs. The solution is based on the recently introduced cavity master equation (CME), a time-closure turning the, in principle, exact dynamic cavity method into a practical method of analysis and of fast simulation. Running CME *once* is of comparable computational complexity as one Monte Carlo run on the same problem. We show that CME correctly models the ferromagnetic p-spin Glauber dynamics from high temperatures down to and below the spinoidal transition. We also show that CME allows an alternative exploration of the low-temperature spin-glass phase of the model.

DOI: 10.1103/PhysRevE.97.050103

Nature abounds in systems of interacting units with nontrivial dynamical properties. This leads to similar questions in condensed-matter physics [1], systems biology [2], neuroscience [3], and neural networks [4] but also in many practical applications in computer science [5] and engineering [6]. Not surprisingly, the study of such systems has led to the development and the use of similar techniques across different scientific communities.

A common starting point is a Markovian dynamics in continuous time of N discrete interacting variables $\underline{\sigma} = \{\sigma_1, \ldots \sigma_N\}$. Such a system is described by a master equation defining the evolution of the probability of the states of the system $P(\underline{\sigma})$ [3,7,8]:

$$\frac{dP(\underline{\sigma})}{dt} = \sum_{\sigma'} [r(\underline{\sigma}' \to \underline{\sigma}) P(\underline{\sigma}') - r(\underline{\sigma} \to \underline{\sigma}') P(\underline{\sigma})], \quad (1)$$

where r are transition probabilities from states and $P(\underline{\sigma})$ depends on time, but for simplicitly, we will not write this dependence explicitly.

The solution of the master equation, Eq. (1), is in general a cumbersome task and exact results on both stationary states and transients are limited to some special cases [3,8–10]. For fully connected [11] and diluted graphs [12] it is possible to resort to hierarchical schemes to derive dynamical equations for the probability of some macroscopic observables. A very general one of this type is the dynamical replica analysis [13–15]. With this reduction of the dimensionality the problem becomes tractable, but one loses the detailed information about the microscopic state of the system and the results are not exact for fully connected [16], nor for the transients in 1D ferromagnetic systems [17].

A frequently made approximation reduces Eq. (1) to a simpler master equation for the probabilities of single-spin variables $P(\sigma_i)$. However, this is only valid in mean-field-like models [3] or at very high temperatures. An alternative solution that successfully describes the local dynamics of these systems in a wide range of the parameter space was recently suggested in Ref. [18]. The problem is then reduced to the solution of a master equation for a conditional probability that is subsequently used to recover $P(\sigma_i)$.

In this work we generalize this last approach to systems with multiparticle interactions and explore its potential to describe processes both near to equilibrium and deep into a phase with multiple minima. We show also that it can be exploited to obtain the ground state of models with a complex energy landscape. To keep the notation simple, and to conveniently explore the features of our solution, we study the diluted ferromagnetic p-spin model with Glauber dynamics. However, the ideas behind our derivation should be clear enough to allow the straightforward application of our method to other dynamical rules and other Hamiltonians.

The ferromagnetic p-spin model is defined by the Hamiltonian

$$H = -\sum_{i_1, i_2, \ldots i_p} J_{i_1 i_2 i_3 \ldots i_p} \sigma_{i_1} \sigma_{i_2} \sigma_{i_3} \ldots \sigma_{i_p}, \quad (2)$$

where $J_{i_1, i_2, \ldots i_p} = 1$ for all p-tuplets in the set of hyperedges of a Bethe lattice and zero otherwise, and $\sigma_i \in \{-1, 1\}$ are binary variables. This model is a natural intermediary between spin glasses and structural glasses. Like the former, it is defined by binary variables and fixed in an infinite lattice. With the latter it shares a crystalline state, the absence of quenched disorder, and a finite range of the interactions.

A standard dynamics for this model uses a single-spin transition rule between states $r(\underline{\sigma} \to \underline{\sigma}') = r_i(\sigma_1, \ldots \sigma_i, \ldots \to \sigma_1, \ldots -\sigma_i, \ldots)$. In addition, we will consider that the transition rate of spin i depends only on the state of the spin and its neighborhood; in this case, all p-tuplets it belongs to. Let us define ∂i as the set of p-tuplets that include spin i and use $\sigma_{\partial i}$ as a notation for the set of spins in ∂i excluding σ_i and denote σ_a as the group of spins forming the p-tuplet a. The transition rate for spin i will be then, for a Glauber dynamics: $r_i(\sigma_i, \sigma_{\partial i}) = \frac{\alpha}{2}[1 - \sigma_i \tanh(\beta \sum_{a \in \partial i} J_a \sigma_{a \setminus i})]$, where α defines the time scale of the problem.

*eaurell@kth.se

†mulet@fisica.uh.cu

 ©2018 American Physical Society

Under these general settings the local dynamics of spin i is described by a local master equation:

$$\frac{dP(\sigma_i)}{dt} = -\sum_{\sigma_{\partial i}} [r_i(\sigma_i,\sigma_{\partial i})P(\sigma_i,\sigma_{\partial i}) - r_i(-\sigma_i,\sigma_{\partial i})P(-\sigma_i,\sigma_{\partial i})]. \quad (3)$$

Equation (3) looks simpler than Eq. (1), but it is not a closed set of equations. To close it we need to resort to proper approximations. In this case we first write $P(\sigma_i,\sigma_{\partial i}) = \prod_{a\in\partial i} P(\sigma_{a\setminus i}|\sigma_i)P(\sigma_i)$, which is exact at equilibrium for trees and random graphs with large loops, and substitute it in Eq. (3). The goal in what follows is to find a proper approximation for the dynamics of the conditional probability $P(\sigma_{a\setminus i}|\sigma_i)$ that substituted back in Eq. (3) makes the calculation of $P(\sigma_i,t)$ straightforward.

We build our equations with the help of the theory of random point processes [7,19], where the dynamics of the spin variable σ_i is encoded in a trajectory $\{X_i\}$ that is parametrized by the number of jumps s_i of the corresponding spin in the studied interval $[t_0,t]$ and the times $\{t_1^i,t_2^i,\ldots,t_{s_i}^i\}$. Very generally for spins interacting through Hamiltonians defined on factor graphs the joint probability density Q of these trajectories can be written as $Q(X_1\ldots X_N) = \prod_{i=1}^N \Phi_i(X_i|X_{\partial i})$, where

$$\Phi_i(X_i|X_{\partial i}) = \prod_{l=1}^{s_i} r_i(\sigma_i(t_l),\sigma_{\partial i}(t_l)) \times \exp\left[-\int_{t_0}^{t} r_i(\sigma_i(\tau),\sigma_{\partial i}(\tau))d\tau\right]. \quad (4)$$

For locally treelike graphs this parametrization leads to a message-passing equation (see Supplemental Material at [20] for a detailed derivation), structurally identical to the belief propagation equations used to approximate an equilibrium Gibbs-Boltzmann distribution [5]:

$$\mu_{a\to(i)}(X_{a\setminus i}|X_i) = \prod_{j\in a\setminus i} \sum_{X_b|b\in\partial j\setminus a} \Phi_j(X_j|X_{\partial j}) \times \prod_{b\in\partial j\setminus a} \mu_{b\to(j)}(X_{b\setminus j}|X_j). \quad (5)$$

Formally, Eq. (5) defines a set of fixed point equations for the probabilities $\mu_{a\to(i)}(X_{a\setminus i}|X_i)$ of the histories in the set $X_{a\setminus i}$ in terms of equivalent objects in the neighborhood of the spins in $a\setminus i$, considering that the history X_i is given. One must notice that this is not the only possible choice. At this point, $\mu_{a\to(i)}(X_i|X_{a\setminus i})$ also looks like a valid alternative to proceed through the derivation in Ref. [18], however, it does not lead to a closed set of equations.

Unfortunately, the histories, defined by the variables X are cumbersome arguments to treat beyond formal statements, and actual solution of Eq. (5) is hopeless. One can, however, marginalize this quantity via $p(\sigma_{a\setminus i}|X_i,t) = \sum_{\substack{X_{a\setminus i}\\ \sigma_{a\setminus i}(t)=\sigma_{a\setminus i}}} \mu_{a\to(i)}(X_{a\setminus i}|X_i)$ and then take the proper time derivative (see Supplemental Material [20]) to obtain

$$\dot{p}(\sigma_{a\setminus i}|X_i) = -\sum_{j\in a\setminus i} \sum_{\substack{\{\sigma_{b\setminus j}\}\\ b\in\partial j\setminus a}} r_j^+ p(\{\sigma_{b\setminus j}\}_{b\in\partial j\setminus a},\sigma_{a\setminus i}|X_i) + \sum_{j\in a\setminus i} \sum_{\substack{\{\sigma_{b\setminus j}\}\\ b\in\partial j\setminus a}} r_j^- p(\{\sigma_{b\setminus j}\}_{b\in\partial j\setminus a},F_j[\sigma_{a\setminus i}]|X_i), \quad (6)$$

where $r_j^{+/(-)} = r_j((-)\sigma_j,\{\sigma_{b\setminus j}\}_{b\in\partial j\setminus a},\sigma_{a\setminus j})$ and $\{\sigma_{b\setminus j}\}$ with $b\in\partial j\setminus a$ is the set of instantaneous variables that characterize the nodes neighboring j, except those in a and $F_j[\sigma_{a\setminus i}]$ is an operator that inverts the sign of spin j in $\sigma_{a\setminus i}$.

Note that although Eq. (6) is exact in treelike graphs, it still contains spin histories as conditional arguments. In principle, these histories could be taken as parameters to be tracked during the solution of Eq. (6). However, it is convenient to go further, assuming first that variables factorize around factor nodes: $p(\{\sigma_{b\setminus j}\}_{b\in\partial j\setminus a},\sigma_{a\setminus i}|X_i) = p(\{\sigma_{b\setminus j}\}_{b\in\partial j\setminus a}|\sigma_{a\setminus i},X_i)p(\sigma_{a\setminus i}|X_i) \approx \prod_{b\in\partial j\setminus a} p(\sigma_{b\setminus j}|\sigma_{a\setminus i})\, p(\sigma_{a\setminus i}|X_i)$, which is exact in treelike graphs in equilibrium. Then, to close the system of equations it is enough to consider that locally the system has short time memory, $p(\sigma|X_i)\sim p(\sigma|\sigma_i)$, which is equivalent to a Markov hypothesis.

With these approximations, Eq. (6) transforms into a master equation but conditioned to neighboring (cavity) spins. We call this the cavity master equation (CME):

$$\dot{p}(\sigma_{a\setminus i}|\sigma_i) = -\sum_{j\in a\setminus i} \sum_{\substack{\{\sigma_{b\setminus j}\}\\ b\in\partial j\setminus a}} r_j^+ \prod_{b\in\partial j\setminus a} p(\sigma_{b\setminus j}|\sigma_j)\; p(\sigma_{a\setminus i}|\sigma_i) + \sum_{j\in a\setminus i} \sum_{\substack{\{\sigma_{b\setminus j}\}\\ b\in\partial j\setminus a}} r_j^- \prod_{b\in\partial j\setminus a} p(\sigma_{b\setminus j}|-\sigma_j)\; p(F_j[\sigma_{a\setminus i}]|\sigma_i). \quad (7)$$

Under very general conditions [18] $p(\sigma_{a\setminus i}|\sigma_i)$ becomes a good proxy for the actual conditional distribution $P(\sigma_{a\setminus i}|\sigma_i)$. Then, to obtain the observables of the system one just solves the set of Eqs. (7), plugs the result in the local master equation, Eq. (3), and integrate to obtain the local probabilities at the nodes of the network. This gives the joint probability distribution of all the variables in every plaquette as a function of time, the same outcome which would require averaging over many realizations using kinetic Monte Carlo (KMC). The numerical integration of Eq. (7) can be done without great difficulty by means of any good numerical integrator such as Runge-Kutta. The integration stepsize affects mainly the running time and has no considerable influence in final results. The natural error accumulation effect for long times is not relevant for the system under study because the long-term behavior of the equations is always stationary. This could be relevant, though, for other systems not reaching equilibrium. Although we will not pursue this issue here, let us note that a similar approach could also, as for standard belief propagation, be used to describe the evolution of the marginal probability of a simply connected subset of nodes in the graph.

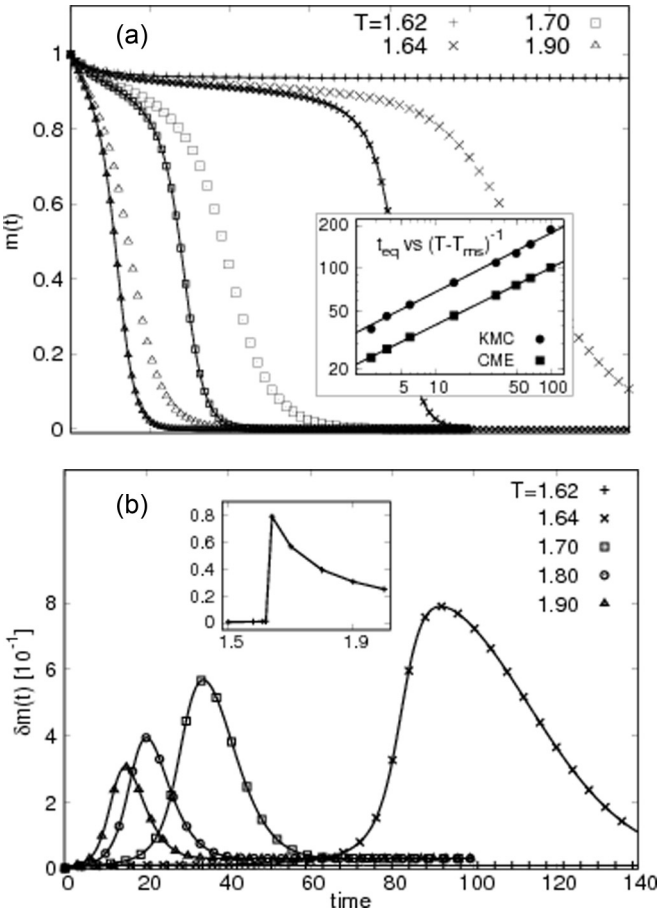

FIG. 1. Top: Dynamics of the average magnetization using CME (lines and symbols) and KMC (symbols). In the inset: Equilibration time near the spinodal transition temperature. Bottom: Dynamical behavior of the local error between CME and KMC. System size: $N = 99\,999$ spins. In the inset: Temperature dependence of the maximum local error. At time $t = 0$ the system is fully magnetized and then begins to interact with a heat bath at a given temperature. KMC curves represent an average over 5000 samples.

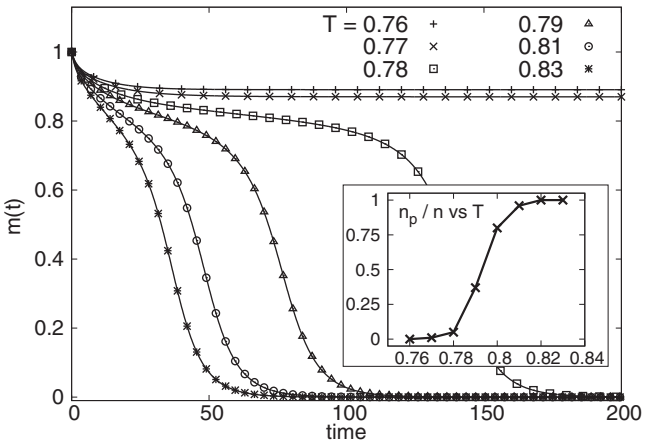

FIG. 2. Dynamical behavior of the planted model for $N = 10\,002$ near T_d. In the plot are represented curves for a single planted graph. In the inset we show the fraction of the samples ($n = 100$) in which the magnetization decays to zero as a function of T.

Let us now discuss in more detail some of the properties of the p-spin ferromagnetic model with $p = 3$ in a random regular graph with $k = 3$. As discussed in Ref. [21] it shows three different phases. For $T > T_{\rm ms} = 1.63$ it is paramagnetic. At $T_{\rm ms}$ emerges a ferromagnetic metastable consistent with a spinodal transition. This ferromagnetic state becomes stable at $T_{\rm fm} = 1.21$. For lower temperatures $T < T_K = 0.655$ [22] the system has a thermodynamic phase transition to a spin-glass state. This spin-glass state can be understood as a result of the competition between the ferromagnetic ground state and the presence of local configurations that guarantee the same (local) energy of the ferromagnetic state but produce frustration. For example, when a spin is down, it puts an effective negative interaction on the other $k - 1 = 2$ neighbors that will act as an effective antiferromagnetic interaction. Since there are many different realizations of such configurations, the interactions may not be fully satisfied because of existing loops leading to fluctuations in the system dynamics and eventually to the spin freeze characteristic of a glassy phase for $T_d < 0.757$ [22].

We know from previous results that the CME fails to predict KMC results deep into the SG phase and for intermediate timescales near second-order phase transitions [18]. Therefore, we will focus first our attention in the behavior of the method around the spinodal transition. We compare CME to KMC starting at $t = 0$ from a totally ordered configuration with magnetization one. Then we observe the evolution of the average magnetization after a quench to a temperature T and quantitatively compare the CME and KMC using the mean-square difference of local magnetizations $\delta m(t) = \sqrt{\frac{1}{N}\sum_i (m_i^{\rm CME}(t) - m_i^{\rm KMC}(t))^2}$.

Results for both quantities are reported in panels of Fig. 1. In this numerical experiment, below the spinodal transition ($T_{\rm ms} < 1.63$), and deep in the high-temperature region ($T > 1.90$) CME and KMC produce similar output. In the first case the system stays trapped in the magnetized state, while in the latter case the system relaxes exponentially to a paramagnetic phase. Only above and near the spinodal transition and at intermediate times do the algorithms differ; the long-term results, however, are also very similar. Note that even around the spinodal transition the errors ultimately become zero supporting the idea that the CME properly reproduces the long-time behavior of the system. The residual error presented in the inset is due to the finite number of samples used and reflects the statistics of the KMC (see Suplemental Materials at [20] for supporting numerical results). One must also remark that these results consider samples where finite-size effects are small on the timescale of interest.

We also tested our CME in a planted model [23] near the dynamical phase transition of the model T_d. The planted model is built fixing the ground state, all $\sigma_i = 1$, and then choosing the value of the links in the graph following the rule: $P(J_a = 1) = \frac{1+\tanh(\beta)}{2}$ and $P(J_a = -1) = \frac{1-\tanh(\beta)}{2}$. The results of the evolution of the magnetization in this graph are shown in Fig. 2. In this case our dynamics evolves toward the correct paramagnetic state for $T > 0.78$ a temperature that is close to but slightly above the expected $T_d = 0.757$. However, one

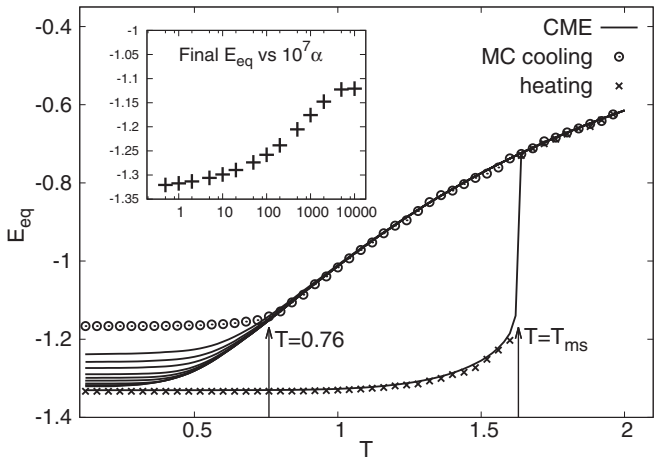

FIG. 3. Comparison between the quasiequilibrium evolution of the CME (continuous lines) and KMC (dots). The CME was applied to a $N = 1002$ system, and KMC to a $N = 10\,002$ system. The temperature step is in both cases $\Delta T = 0.02$. Both approaches reproduce the existence of $T_{\rm ms} \approx 1.62$. Below T_d both dynamics differentiate.

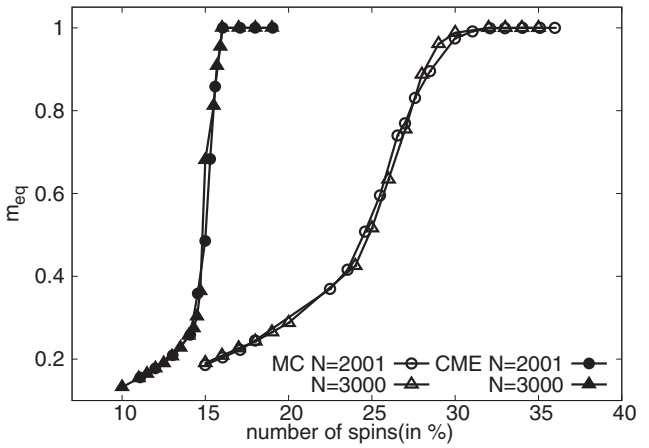

FIG. 4. Final magnetization of a system as a function of the number of fixed spins at $T = 0.12$ following the dynamics of the CME $N = 2001$ and KMC $N = 3000$. The symbols represent the average over 100 configurations of the local fields.

most notice that these results are strongly affected by sample to sample fluctuations, as the inset in Fig. 2 shows.

Motivated by the long-time behavior of the CME we explored the behavior of the observables of the system in an adiabatic protocol. Although the set of differential Eqs. (7) was written with the aim to study dynamical processes one can also make the system evolve to see if it reaches a fixed point. This idea is used here to reproduce adiabatic heating and cooling experiments in the model. In Fig. 3 we show the result of these experiments and compare them with KMC. The heating process reflects quite well the existence of $T_{\rm ms}$. Starting from an homogeneous ferromagnetic configuration at low T, the temperature is increased in small steps. Both CME and KMC remain in the ferromagnetic state until it disappears beyond the spinodal temperature and then jumps to the paramagnetic state.

However, if we start cooling the system from a paramagnetic state at high temperatures (Fig. 3), the CME and KMC will coincide only down to the temperature $T_d \approx 0.757$ for which the spin-glass phase dynamically traps the stochastic simulation [21]. Below this temperature the behavior of the CME depends on the criterion adopted to define the convergence of the algorithm. Our criterion is to stop whenever for each plaquette $|p(\sigma_k,\sigma_j|\sigma_i,t+dt) - p(\sigma_k,\sigma_j|\sigma_i,t)| \leqslant \delta$, where δ is a parameter controlling the time that the system spends at a given temperature. The smaller the δ the larger the time we gave the system to equilibrate. Remarkably, if δ is small enough the overall energy value obtained at the end of the cooling experiment is very close to the ferromagnetic prediction. In this case the final probability distribution in each plaquette weighs equally the four states that satisfying the local interactions. As a consequence of symmetry, the local magnetization is then zero. This suggests that the CME is averaging out the glassy states in this regime.

This low temperature structure is indeed one of the most interesting features of the model, since despite the clear presence of a crystalline state it cannot be reached by any known local dynamical rule. In that scenario, we decided to fix a fraction of the spins using strong local fields pointing in the same direction. We then inquired how large should be the fraction of spins aligned to obtain the correct crystalline state after a quench to a very low temperature. The results are shown in Fig. 4. KMC dynamics converges to the proper equilibrium state when almost 30% of the spin are oriented in the ferromagnetic state, while the pseudodynamics of the CME at low temperature recognize the ground state of the model with only a 15% of the spins correctly oriented. The smaller number of spins needed to drive the dynamics of the model into the ground state of the system for the CME suggests that it can be used as proper proxy for similar problems in combinatorial optimization.

In summary, we have presented a formal approach to study the continuous dynamics of a discrete system with multiple-particle interactions. We illustrate the power of this approach studying the dynamical behavior of the p-spin diluted ferromagnet. We have shown that the cavity master equation reproduces the long-time behavior of kinetic Monte Carlo simulations in a wide temperature range. CVM also reproduces exactly the spinodal temperature $T_{\rm ms}$ and provides a very good approximation for the exact value of the dynamical temperature T_d. Below T_d, where the spin-glass states dominate the dynamics the CME fails to predict the KMC results. However, this allows a deeper exploration of the structure of the glassy phase and in particular to find the ground state of the system by fixing a small number of spins.

This project has received funding from the European Union's Horizon 2020 research and innovation programme MSCA-RISE-2016 under Grant Agreement No. 734439 INFERNET. It has been partially supported by the STINT (Sweden) project "Enhancing cooperation opportunities with Havana University through the Erasmus Programme actions," by an Erasmus+ International Credit Mobility to KTH (EU), and by the COIN Centre of Excellence of the Academy of Finland (Grant No. 251170).

[1] A. Onuki, *Phase Transition Dynamics* (Cambridge University Press, Cambridge, UK, 2002).
[2] M. Nowak, *Evolutionary Dynamics: Exploring the Equations of Life* (The Belknap Press, Cambridge, MA, 2006).
[3] D. Amit, *Modelling Brain Function: The World of Attractor Neural Networks* (Cambridge University Press, Cambridge, UK, 1989).
[4] K. Gurney, *An Introduction to Neural Networks* (University College of London, London, 1999).
[5] M. Mezard and A. Montanari, *Information, Physics, and Computation* (Oxford University Press, Oxford, 2009).
[6] S. J. Schiff, *Neural Control Engineering* (The MIT Press, Cambridge, MA, 2011).
[7] N. G. van Kampen, *Stochastic Processes in Physics and Chemistry* (Elsevier, Amsterdam, 1992), Vol. 1.
[8] A. C. C. Coolen, R. Kühn, and P. Sollich, *Theory of Neural Information Processing Systems* (Oxford University Press, Oxford, 2005).
[9] R. J. Glauber, Time-dependent statistics of the Ising model, J. Math. Phys. **4**, 294 (1963).
[10] P. Mayer and P. Sollich, General solutions for multispin two-time correlation and response functions in the Glauber–Ising chain, J. Phys. A **37**, 9 (2004).
[11] S. N. Laughton, A. C. C. Coolen, and D. Sherrington, Order-parameter flow in the SK spin-glass: I. Inclusion of microscopic memory effects, J. Phys. A **29**, 763 (1996).
[12] G. Semerjian and M. Weigt, Approximation schemes for the dynamics of diluted spin models: The Ising ferromagnet on a Bethe lattice, J. Phys. A **37**, 5525 (2004).
[13] J. P. L. Hatchett, I. Pérez-Castillo, A. C. C. Coolen, and N. S. Skantzos, Dynamical replica analysis of disordered Ising spin systems on finitely connected random graph, Phys. Rev. Lett. **95**, 117204 (2005).
[14] A. Mozeika and A. C. C. Coolen, Dynamical replica analysis of processes on finitely connected random graphs: I. vertex covering, J. Phys. A **41**, 115003 (2008).
[15] A. Mozeika and A. C. C. Coolen, Dynamical replica analysis of processes on finitely connected random graphs: I. Dynamics in the Griffiths phase of the diluted Ising ferromagnet, J. Phys. A **42**, 195006 (2009).
[16] H. Nishimori and M. Yamana, Dynamical probability distribution function of the SK model at high temperatures, J. Phys. Soc. Jpn. **65**, 3 (1996).
[17] G. D. Ferraro and E. Aurell, Perturbative large deviation analysis of non-equilibrium dynamics, J. Phys. Soc. Jpn. **83**, 084001 (2014).
[18] E. Aurell, G. D. Ferraro, E. Domínguez, and R. Mulet, A cavity master equation for the continuous time dynamics of discrete spins model, Phys. Rev. E **95**, 052119 (2017).
[19] C. Kipnis and C. Landim, *Scaling Limits of Interacting Particle Systems* (Springer Verlag, Berlin, 1999), Vol. 320.
[20] See Supplemental Material at http://link.aps.org/supplemental/10.1103/PhysRevE.97.050103 for a detailed derivation of the message-passing equation.
[21] S. Franz, M. Mézard, and F. Ricci-Tersenghi, A ferromagnet with a glass transition, Europhys. Lett. **55**, 465 (2001).
[22] A. Montanari and F. Ricci-Tersenghi, Cooling-schedule dependence of the dynamics of mean-field glasses, Phys. Rev. B **70**, 134406 (2004).
[23] L. Zdeborová and F. Krzakala, Statistical physics of inference: Thresholds and algorithms, Adv. Phys. **65**, 453 (2016).